

表 3. PEG-rHSA の物性

	rHSA	PEG(5kDa)-rHSA	PEG(10kDa)-rHSA
Mw	66500	136500	186500
R _h	3.05	6.73	8.85
[rHSA](wt%)	1.34	5.00	1.34
Viscosity(cP) at 3160 s ⁻¹	0.67	0.95	3.00
COP(mmHg)	3.1	17.2	63.3

した。膠質浸透圧(COP)はコロイド浸透圧計(MWCO:30 kDa)にて測定した。

PEG-rHSA の血漿増量剤としての有効性を評価するため、出血性ショックモデルラットを作製し、出血性ショック状態からの輸液による蘇生効果を検討した。実験対象は Wistar 雄性ラット(6~7 週齢, 日本クレアより購入)を一晩絶食にしたものを用いた。ジエチルエーテルにより麻酔導入後、イソフルランにて全身麻酔し、仰臥位に固定した。直腸温センサーにより体温をモニターし、接続したヒーティングランプの照射により体温を維持した。また、左大腿動脈にカニューレーションを行い、血圧測定に用いた。右大腿動脈および大腿静脈にカニューレーションを行い、それぞれ脱血および輸液用のラインを接続した。血圧が約 80 mmHg となるように麻酔濃度を調節し、安定させた後、全血液量(56 mL/kg と仮定)の 40%を 5 分かけて脱血し、ショック状態とした。脱血終了から 30

分間に脱血量と同量の輸液を 5 分かけて投与し、その後 3 時間、血圧の変化を観察した。また、輸液投与の 5 分前と投与終了後 30 分後に右大腿動脈から約 100 μL 採血し、血液ガスを測定した。

結果・考察

粘度計を用いて粘性を評価した結果、rHSA に PEG を結合させることにより流体力学半径を大きくすることができ、更に粘度や膠質浸透圧も大きく向上させることが明らかになった(表 4)。

脱血後には血圧は 20~35 mmHg まで下降し、その後緩やかに上昇傾向を見せた。これは血圧の下降に伴って相対的に膠質浸透圧の効果が高まり、血管内に水を引き込んで血圧を回復したことによると考えられる。輸液を投与することで、速やかに血圧は上昇し、その後、緩やかに下降した(図 16)。輸液直後の血圧の上昇に差

表 4 出血性ショックラットの血液ガスの測定

	Baseline	25min after Shock	30min after Resuscitation					
			rHSA 1.34 %	rHSA 5 %	PEG(5kDa)-rHSA 1.34 %	PEG(10kDa)-rHSA 0.67 %	PEG(10kDa)-rHSA 1.34 %	
pH	7.34 ± 0.04	7.28 ± 0.08 †	7.33 ± 0.08 †	7.35 ± 0.06	7.32 ± 0.06	7.35 ± 0.04	7.35 ± 0.06	
BE(mmol/L)	2.2 ± 1.9	-8.5 ± 3.0 †	-1.5 ± 1.3 †	-2.0 ± 3.4 †	-4.3 ± 7.4	0.7 ± 0.6 †	3.0 ± 2.8 †	
PaO ₂ (mmHg)	65.9 ± 13.0	85.4 ± 6.2 †	78.5 ± 9.9	67.3 ± 10.1 †	73.0 ± 3.6	72.7 ± 4.5	63.5 ± 10.6 †	
PaCO ₂ (mmHg)	51.8 ± 4.5	38.9 ± 2.8 †	47.1 ± 11.2	42.7 ± 10.7 †	41.1 ± 6.7	46.9 ± 6.4	51.9 ± 13.9	
HCO ₃ ⁻ (mmol/L)	27.9 ± 1.6	18.2 ± 2.2 †	24.5 ± 0.8 †	23.7 ± 3.5 †	21.7 ± 6.2	26.0 ± 1.2 †	28.2 ± 3.8 †	
tCO ₂ (mmol/L)	29.4 ± 2.0	19.4 ± 2.6 †	26.0 ± 1.0 †	25.0 ± 3.6 †	23.0 ± 6.2	27.3 ± 1.5 †	30.0 ± 4.2 †	
Na(mmol/L)	138 ± 1	134 ± 4 †	135 ± 0 †	138 ± 3	135 ± 2	137 ± 1	137 ± 1 †	
K(mmol/L)	3.9 ± 0.4	5.8 ± 1.8 †	5.5 ± 0.6	5.1 ± 1.4	6.5 ± 1.1	4.6 ± 0.3	5.3 ± 0.1	
iCa(mmol/L)	1.25 ± 0.02	1.30 ± 0.05	1.43 ± 0.01	1.23 ± 0.07	1.25 ± 0.17	1.36 ± 0.09	1.31 ± 0.18	
Hct(%)	43.5 ± 2.8	33.3 ± 6.5 †	21.5 ± 3.4 †	23.3 ± 5.2 †	23.0 ± 3.5 †	23.7 ± 2.1 †	23.0 ± 1.4 †	

† P < 0.05 compared to Baseline

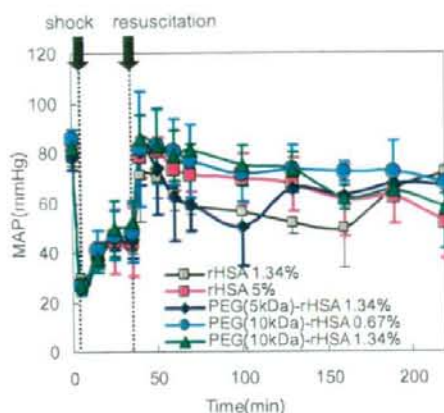


図 16 出血性ショックモデルラットの血圧の測定

はみられるものの、輸液3時間後にはいずれもほぼ同じ値となった。1.34%のrHSAを投与したものは3時間以内でも80%程の高い死亡率となったが、5%のrHSAを投与した場合は全例が生じた。PEG(10kDa)-rHSAを投与した場合も高い生存率が得られた。よって出血性ショック状態の回復には膠質の投与が有効であることが明らかとなった。

血液ガスの測定結果を表4に示した。Hct値はおよそ23%に低下し、置換モデルとして有効であることが分かる。ショック時には循環血液量が不足するため、BEが大きくマイナスに傾き、顕著なアシドーシスを示したが、輸液の投与後はいずれの場合も概ね改善する傾向をみせた。

これらの結果から、出血性ショック時にPEG-rHSAを投与した場合にはrHSAを投与した場合と比較して、より少ない濃度でもほぼ同様の効果が得られるであろうことが示された。

結論

血圧の測定、血液ガスの測定から、出血性ショックモデルにおいて、PEG-rHSAはrHSAと

比較して少ない濃度で状態を回復させ維持できることが示された。今後、最適な輸液量を決定するために更なる検討が必要である。

D. 考察

本研究は「PEG-rHSAを救急救命で使用可能な酸素供給補助製剤」として確立することを目的とし、マテリアルの確立および生体計測の両側面からアプローチした。まず製剤の安定した製造法を確立し、物性評価から安定性を確認し、またその保存方法を確立した。生体内投与による実質的有効性を検討する前臨床試験では、脳微小循環のNOイメージングから出血性ショックモデルにおいてPEG-rHSAは血液粘度を維持することで血管のNO生成量を増加させ、血管を拡張させるために有効であることを証明した。組織のエネルギー代謝の側面から検討すべく心臓および肝臓のメタボローム解析を試みた結果、ショックからのエネルギー回復に関しては対照群同等に維持され、酸化還元バランスも良好であることが示され、また血液ガス分析結果もそれを支持するものであった。一方、当初仮説を立てた止血効果の増強に関しては実験結果からPEG-rHSAは止血機序を抑制する効果があることが明らかになり、臨床応用には留意すべき点も明らかになった。これは今後メカニズムを明らかにすることで、新たな血栓形成の分子メカニズムの解明にも繋げると期待できる。最終的には霊長類への投与を実施し、さらなる安全性を確認する必要がある。

D. 結論

救命救急への応用を目的とした安全かつ効果的な輸液製剤であるPEG-rHSAを新たに開発した。PEG-rHSAは組織への酸素輸送を維持し、臓器の代謝を維持することを示した。PEG-rHSA人工酸素運搬体としての可能性を示すに至った。

E. 健康危険情報

特になし。

F. 研究発表

F-1 論文発表

末松 誠

- Kinoshita, A., Tsukada, K., Soga, T., Hishiki, T., Ueno, Y., Nakayama, Y., Tomita, M., Suematsu, M.: Roles of hemoglobin allosteric in hypoxia-induced metabolic alterations in erythrocytes: simulation and its verification by metabolome analysis, *J. Biol. Chem.*, 282(14), 10731-10741, 2007.
- Soga, T., Baran, R., Suematsu, M., Ueno, Y., Ikeda, S., Sakurakawa, T., Kakazu, Y., Ishikawa, T., Robert, M., Nishioka, T. Tomita, M.: Differential metabolomics reveals ophthalmic acid as an oxidative stress biomarker indicating hepatic glutathione consumption. *The Journal of biological chemistry*, 281(24), 16768-16776, 2006.
- Saganuma, K., Tsukada, K., Tsuneshige, A., Kashiba, M., Yonetani, T., Suematsu, M.: Erythrocytes with T-state-stabilized hemoglobin as a therapeutic tool for postischemic liver dysfunction., *Antioxidants & redox signaling*, 8, 1847-1855, 2006.
- 末松 誠, 菱木貴子, 岩淵拓也, 山本雄広, 行武良哲, 塚田孝祐: メタボローム解析技術による新しい代謝制御機構の系統的探索: ガスバイオロジーの推進と医学への応用, *細胞工学*, 25(12), 1427-1431, 2006.
- Ishikawa, H., Naito, T., Iwanaga, T., Takahashi-Iwanaga, H., Suematsu, M., Hibi, T., Nanno, M.: Curriculum vitae of intestinal intraepithelial T cells: Their developmental and behavioral characteristics. *Immunological reviews*, 215(1), 154-165, 2007.
- Miyao, N., Suzuki, Y., Takeshita, K., Kudo, H., Ishii, M., Hiraoka, R., Nishio, K., Tamatani, T., Sakamoto, S., Suematsu, M., Tsumura, H., Ishizaka, A., Yamaguchi, K.: Various adhesion molecules impair microvascular leukocyte kinetics in ventilator-induced lung injury., *American journal of physiology. Lung cellular and molecular physiology*, 290, L1059-L1068, 2006.
- Yamashita, T., Shoge, M., Oda, E., Yamamoto, Y., Giddings, J.C., Kashiwagi, S., Suematsu, M., Yamamoto, J.: The free radical scavenger, edaravone, augments NO release from vascular cells and platelets after laser-induced acute endothelial injury in vivo., *Platelets*, 17, 201-206, 2006.
- Higuchi, A., Ueno, R., Shimmura, S., Suematsu, M., Dogru, M., Tsubota, K.: Albumin rescues ocular epithelial cells from cell death in dry eye. *Curr. Eye Res.*, 32(2), 83-88, 2007.
- Hangai-Hoger, N., Tsai, A.G., Carbales, P., Suematsu, M., Intaglietta, M.: Microvascular and systemic effects following top load administration of saturated carbon monoxide-saline solution, *Crit. Care Med.*, 35(4), 1123-1132, 2007.
- Adachi, T., Yamamoto, M., Suematsu, M.: Targeting NAD(P)H oxidase: Ets-1 regulates p47phox expression, *Circ. Res.*, 101, 962-964, 2008.
- Shintani, T., Iwabuchi, T., Soga, T., Kato, Y., Yamamoto, T., Takano, N., Hishiki, T., Ueno, Y., Ikeda, S., Sakuragawa, T., Ishikawa, K., Goda, N., Kitagawa, Y., Kajimura, M., Matsumoto, K., Suematsu, M.: Cystathionine β -synthase as a carbon monoxide-sensitive regulator of bile excretion., *Hepatology*, 49, 141-150, 2009

塚田孝祐

- Kinoshita, A., Tsukada, K., Soga, T., Hishiki, T., Ueno, Y., Nakayama, Y., Tomita, M., Suematsu, M.: Roles of hemoglobin allosteric in hypoxia-induced metabolic alterations in erythrocytes: simulation and its verification by metabolome analysis, *J. Biol. Chem.*, 282(14), 10731-10741, 2007.

- Suganuma, K., Tsukada, K., Tsuneshige, A., Kashiba, M., Yonetani, T., Suematsu, M.: Erythrocytes with T-state-stabilized hemoglobin as a therapeutic tool for postischemic liver dysfunction., *Antioxidants & redox signaling*, 8, 1847-1855, 2006.

中城圭介

- Kragh-Hansen U, Watanabe H, Nakajou K., Iwao Y, Otagiri M.: Chain length-dependent binding of fatty acid anions to human serum albumin studied by site-directed mutagenesis, *J. Mol. Biol.*, 363, 702-712, 2006.
- Iwao Y, Anraku M, Hiraike M, Kawai K, Nakajou K., Kai T, Suenaga A, Otagiri M.: The structural and pharmacokinetic properties of oxidized human serum albumin, advanced oxidation protein products (AOPP), *Drug Metab. Pharmacokinet.*, 21(2), 140-146, 2006.
- Nakano N, Fukuhara-Takaki K, Jono T, Nakajou K., Eto N, Horiuchi S, Takeya M, Nagai R.: Association of advanced glycation end products with A549 cells, a human pulmonary epithelial cell line, is mediated by a receptor distinct from the scavenger receptor family and RAGE, *J. Biochem.*, 139, 821-829, 2006.
- Katayama N., Nakajou K., Komori H., Uchida K., Yokoe JI, Yasui N., Yamamoto H., Kai T., Sato M., Nakagawa T., Takeya M., Maruyama T., Otagiri M.: Design and evaluation of S-nitrosylated human serum albumin (SNO-HSA) as a novel anticancer drug, *The Journal of Pharmacology and Experimental Therapeutics*, 325(1), 69-76, 2008
- Nagai R, Mera K., Nakajou K., Fujiwara Y., Iwao Y., Imai H., Murata T., Otagiri M.: The ligand activity of AGE-proteins to scavenger receptors is dependent on their rate of modification by AGEs, *Biochimica et Biophysica Acta*, 1772, 1192-1198, 2007
- Iwao Y., Nakajou K., Nagai R., Kitamura K., Anraku M., Maruyama T., Otagiri M.: CD36 is one of important receptors promoting renal tubular injury by ad-

vanced oxidation protein products., *American Journal of Physiology-Renal Physiology*. In press.

竹内良人

- 特になし

片山富博

- 特になし

Ryon Bateman

- Bateman RM., Sharpe MD, Goldman D, Lidington D and Ellis CG: Inhibiting Nitric Oxide Overproduction during Hypotensive Sepsis increases local oxygen consumption in Rat Skeletal Muscle., *Crit Care Med.*, 36(1), 225-231, 2008.
- Boyd JH, Chau EH, Tokunaga CT, Bateman RM., Haljan G, Davani ES, Wang Y, Walley KR.: Fibrinogen decreases cardiomyocyte contractility through an ICAM-1 dependent mechanism., *Critical Care*, 12(1), R2, 2008.
- Bateman RM., Ohmura M, Nagahata Y, Hishiki T and Suematsu M.: Endotoxemia induces an early differential metabolic response in the heart and liver as determined by metabolomic analysis., *Critical Care*, 12(2), S155, 2008
- Bateman RM., Obata R, Nagahata Y, Ohmura M, Hishiki T, Suematsu M.: Endotoxemia induces a differential metabolic response in the heart and liver as determined by metabolomic analysis, *Experimental Biology*, 2009.

G. 知的財産権の出願・登録状況

なし。

H. 他の研究との関連

本研究におけるメタボローム解析法の確立および設備の導入に関しては文部科学省リーディングプロジェクト細胞・生体機能シミュレーションプロジェクト (H15~H19) によって行われた。

II 研究成果の刊行に関する一覧表

研究成果の刊行に関する一覧表

雑誌

発表者名	論文タイトル名	発表誌名	巻名	ページ	出版年
Kinoshita, A., <u>Tsukada, K.</u> , Soga, T., Hishiki, T., Ueno, Y., Nakayama, Y., Tomita, M., <u>Suematsu, M.</u>	Roles of hemoglobin allostery in hypoxia-induced metabolic alterations in erythrocytes: simulation and its verification by metabolome analysis	J. Biol. Chem.	282(14)	10731-10741	2007
Soga, T., Baran, R., <u>Suematsu, M.</u> , Ueno, Y., Ikeda, S., Sakurakawa, T., Kakazu, Y., Ishikawa, T., Robert, M., Nishioka, T., Tomita, M.	Differential metabolomics reveals ophthalmic acid as an oxidative stress biomarker indicating hepatic glutathione consumption.	The Journal of biological chemistry	281(24)	16768-16776	2006
Suganuma, K., <u>Tsukada, K.</u> , Tsuneshige, A., Kashiba, M., Yonetani, T., <u>Suematsu, M.</u>	Erythrocytes with T-state-stabilized hemoglobin as a therapeutic tool for post-ischemic liver dysfunction.	Antioxidants & redox signaling	8	1847-1855	2006
末松 誠, 菱木貴子, 岩淵拓也, 山本雄広, 行武良哲, 塚田孝祐	メタボローム解析技術による新しい代謝制御機構の系統的探索:ガスバイオロジーの推進と医学への応用	細胞工学	25(12)	1427-1431	2006
Ishikawa, H., Naito, T., Iwanaga, T., Takahashi-Iwanaga, H., <u>Suematsu, M.</u> , Hibi, T., Nanno, M.	Curriculum vitae of intestinal intraepithelial T cells: Their developmental and behavioral characteristics.	Immunological reviews	215(1)	154-165	2007
Miyao, N., Suzuki, Y., Takeshita, K., Kudo, H., Ishii, M., Hiraoka, R., Nishio, K., Tamatani, T., Sakamoto, S., <u>Suematsu, M.</u> , Tsunemura, H., Ishizaka, A., Yamaguchi, K.	Various adhesion molecules impair microvascular leukocyte kinetics in ventilator-induced lung injury.	American journal of physiology. Lung cellular and molecular physiology	290	L1059-L1068	2006

Yamashita, T., Shoge, M., Oda, E., Yamamoto, Y., Giddings, J.C., Kashiwagi, S., <u>Suematsu, M.</u> , Yamamoto, J.	The free radical scavenger, edaravone, augments NO release from vascular cells and platelets after laser-induced acute endothelial injury in vivo.	Platelets	17	201-206	2006
Kragh-Hansen U, Watanabe H, <u>Nakajou K</u> , Iwao Y, Otagiri M.	Chain length-dependent binding of fatty acid anions to human serum albumin studied by site-directed mutagenesis	J. Mol. Biol.	363	702-712	2006
Iwao Y, Anraku M, Hiraike M, Kawai K, <u>Nakajou K</u> , Kai T, Suenaga A, Otagiri M.	The structural and pharmacokinetic properties of oxidized human serum albumin, advanced oxidation protein products (AOPP)	Drug Metab. Pharmacokinet.	21(2)	140-146	2006
Nakano N, Fukuhara-Takaki K, Jono T, <u>Nakajou K</u> , Eto N, Horiuchi S, Takeya M, Nagai R.	Association of advanced glycation end products with A549 cells, a human pulmonary epithelial cell line, is mediated by a receptor distinct from the scavenger receptor family and RAGE	J. Biochem	139	821-829	2006
Higuchi, A., Ueno, R., Shimamura, S., <u>Suematsu, M.</u> , Dogru, M., Tsubota, K.	Albumin rescues ocular epithelial cells from cell death in dry eye	Curr. Eye Res.	32(2)	83-88	2007
Hangai-Hoger, N., Tsai, A.G., Carbales, P., <u>Suematsu, M.</u> , Intaglietta, M.	Microvascular and systemic effects following top load administration of saturated carbon monoxide-saline solution	Crit. Care Med.	35(4)	1123-1132	2007
Adachi, T., Yamamoto, M., <u>Suematsu, M.</u>	Targeting NAD(P)H oxidase: Ets-1 regulates p47phox expression	Circ. Res.	101	962-964	2008

Katayama N., <u>Nakajou K.</u> , Komori H., Uchida K., Yokoe JI., Yasui N., Yamamoto H., Kai T., Sato M., Nakagawa T., Takeya M., Maruyama T., Otagiri M.	Design and evaluation of S-nitrosylated human serum albumin (SNO-HSA) as a novel anticancer drug	The Journal of Pharmacology and Experimental Therapeutics	325(1)	69-76	2008
Nagai R., Mera K., <u>Nakajou K.</u> , Fujiwara Y., Iwao Y., Imai H., Murata T., Otagiri M.	The ligand activity of AGE-proteins to scavenger receptors is dependent on their rate of modification by AGEs	Biochimica et Biophysica Acta	1772	1192-1198	2007
Shintani, T., Iwabuchi, T., Soga, T., Kato, Y., Yamamoto, T., Takano, N., Hishiki, T., Ueno, Y., Ikeda, S., Sakuragawa, T., Ishikawa, K., Goda, N., Kitagawa, Y., Kajimura, M., Matsumoto, K., <u>Suematsu, M.</u>	Cystathionine β -synthase as a carbon monoxide-sensitive regulator of bile excretion.	Hepatology	49	141-150	2009
<u>Bateman RM.</u> , Sharpe MD, Goldman D, Lidington D and Ellis CG	Inhibiting Nitric Oxide Overproduction during Hypotensive Sepsis increases local oxygen consumption in Rat Skeletal Muscle.	Crit Care Med.	36(1)	225-231	2008
Boyd JH, Chau EH, Tokunaga CT, <u>Bateman RM.</u> , Haljan G, Davani ES, Wang Y, Walley KR.	Fibrinogen decreases cardiomyocyte contractility through an ICAM-1 dependent mechanism.	Critical Care.	12(1)	R2	2008
<u>Bateman RM.</u> , Ohmura M, Nagahata Y, Hishiki T and <u>Suematsu M.</u>	Endotoxemia induces an early differential metabolic response in the heart and liver as determined by metabolomic analysis.	Critical Care	12(2)	S155	2008
<u>Bateman RM.</u> , Obata R, Nagahata Y, Ohmura M, Hishiki T, <u>Suematsu M.</u>	Endotoxemia induces a differential metabolic response in the heart and liver as determined by metabolomic analysis	Experimental Biology	-	-	2009
Iwao Y., <u>Nakajou K.</u> , Nagai R., Kitamura K., Anraku M., Maruyama T., Otagiri M.	CD36 is one of important receptors promoting renal tubular injury by advanced oxidation protein products.	American Journal of Physiology-Renal Physiology	-	In press	-

III 研究成果の刊行物・別刷

Roles of Hemoglobin Allostery in Hypoxia-induced Metabolic Alterations in Erythrocytes

SIMULATION AND ITS VERIFICATION BY METABOLOME ANALYSIS^{*,3}

Received for publication, November 20, 2006, and in revised form, January 29, 2007. Published, JBC Papers in Press, February 8, 2007, DOI 10.1074/jbc.M610717200

Ayako Kinoshita¹, Kosuke Tsukada², Tomoyoshi Soga¹, Takako Hishiki^{1,2}, Yuki Ueno¹, Yoichi Nakayama¹, Masaru Tomita¹, and Makoto Suematsu^{1,3}

From the ¹Institute for Advanced Biosciences, Keio University, Tsuruoka, Yamagata 997-0017, Japan and ²Department of Biochemistry and Integrative Medical Biology, School of Medicine, Keio University, Shinanomachi, Shinjuku-ku, Tokyo 160-8582, Japan

When erythrocytes are exposed to hypoxia, hemoglobin (Hb) stabilizes in the T-state by capturing 2,3-bisphosphoglycerate. This process could reduce the intracellular pool of glycolytic substrates, jeopardizing cellular energetics. Recent observations suggest that hypoxia-induced activation of glycolytic enzymes is correlated with their release from Band III (BIII) on the cell membrane. Based on these data, we developed a mathematical model of erythrocyte metabolism and compared hypoxia-induced differences in predicted activities of the enzymes, their products, and cellular energetics between models with and without the interaction of Hb with BIII. The models predicted that the allostery-dependent Hb interaction with BIII accelerates consumption of upstream glycolytic substrates such as glucose 6-phosphate and increases downstream products such as phosphoenolpyruvate. This prediction was consistent with metabolomic data from capillary electrophoresis mass spectrometry. The hypoxia-induced alterations in the metabolites resulted from acceleration of glycolysis, as judged by increased conversion of [¹³C]glucose to [¹³C]lactate. The allostery-dependent interaction of Hb with BIII appeared to contribute not only to maintenance of energy charge but also to further synthesis of 2,3-bisphosphoglycerate, which could help sustain stabilization of T-state Hb during hypoxia. Furthermore, such an activation of glycolysis was not observed when Hb was stabilized in R-state by treating the cells with CO. These results suggest that Hb allostery in erythrocytes serves as an O₂-sensing trigger that drives glycolytic acceleration to stabilize intracellular energetics and promote the ability to release O₂ from the cells.

Erythrocytes deliver molecular oxygen (O₂) to tissues through allosteric regulation of hemoglobin (Hb). The ability of Hb to release O₂ is determined by a variety of metabolites in the intracellular compartment, such as protons (H⁺), 2,3-bisphosphoglycerate (2,3-BPG), nitric oxide (NO), and ATP. The decrease in H⁺ and the increase in the aforementioned compounds (2,3-BPG, NO, and ATP) stabilize the T-state of Hb, thereby facilitating O₂ dissociation from the cells. In contrast, O₂ and carbon monoxide (CO) function as positive allosteric effectors that stabilize Hb in its R-state and down-regulate O₂ dissociation. When exposed to hypoxic conditions, erythrocytes are known to accelerate glucose consumption (1). This event appears to result from acceleration of glycolysis, as judged by the increase in 2,3-BPG (2), a metabolite stabilizing the T-state of Hb. Because T-state Hb has a higher affinity to 2,3-BPG and ATP than the R-state Hb, stabilization of the former structure would reduce amounts of free ATP available for maintenance of cellular homeostasis. ATP is consumed continuously by various ATPases to maintain ionic homeostasis and by adenylate cyclase to generate cyclic AMP to maintain the deformability of the cells. Upon hypoxia, a fraction of the intracellular ATP is released to the extracellular space to elicit hypoxia-induced vasorelaxation, although the actual amounts of ATP released seem small compared with levels within the cell (3). Furthermore, the cells require ATP in the initial steps of glycolysis (e.g. used by hexokinase (HK) and phosphofructokinase (PFK)) to trigger ATP synthesis. These features have led researchers to hypothesize that erythrocytes might have mechanisms for responding quickly to hypoxia to up-regulate *de novo* ATP synthesis.

There is a growing body of evidence showing that the interaction of Hb with Band III (BIII), a major transmembrane protein in erythrocytes, plays a role in these compensatory mechanisms to maintain intracellular ATP levels (4–6). BIII, also known as anion exchanger type I, accounts for about 25% of the total erythrocyte membrane protein (7), and its cytoplasmic domain displays a greater affinity for Hb

^{*}This work was supported by JSPS Grant-in-aid for Creative Scientific Research Grant 17GS0419 and in part by a grant from New Energy and Industrial Technology Development Organization. Development of the basic software (E-Cell) was supported by grants from Japan Science and Technology Corp. and from Yamagata Prefecture. Development of computer-based biosimulation for erythrocyte metabolism was supported by Leading Project for Biosimulation from MEXT. The costs of publication of this article were defrayed in part by the payment of page charges. This article must therefore be hereby marked "advertisement" in accordance with 18 U.S.C. Section 1734 solely to indicate this fact.

³The on-line version of this article (available at <http://www.jbc.org>) contains supplemental material.

¹Research associate supported by 21st Century Center-of-Excellence Program from the Ministry of Education, Culture, Sports, Science, and Technology.

²Research fellow supported by Grant-in-aid for Creative Scientific Research Grant 17GS0419.

³To whom correspondence should be addressed. E-mail: m-suematsu@sc.itc.keio.ac.jp.

⁴The abbreviations used are: 2,3-BPG, 2,3-bisphosphoglycerate; CE-MS, capillary electrophoresis mass spectrometry; PK, pyruvate kinase; HK, hexokinase; PFK, phosphofructokinase; ALD, aldolase; GAPDH, glyceraldehyde-3-phosphate dehydrogenase; LDH, lactate dehydrogenase; G6P, glucose 6-phosphate; F6K, fructose 6-phosphate; DHAP, dihydroxyacetone phosphate; 3PG, 3-phosphoglycerate; PEP, phosphoenolpyruvate; F1,6BP, fructose 1,6-bisphosphate; BIII, Band III.

A Hypoxia-responsive Model of Erythrocyte Metabolism

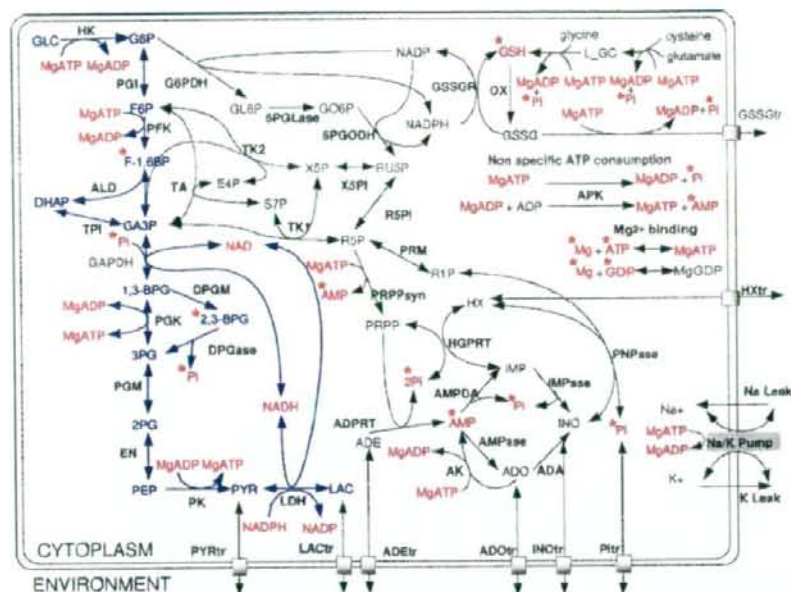


FIGURE 1. Metabolic pathways included in the mathematical model. Blue, glucose-derived carbon flux in glycolysis. Red, substrates or allosteric effectors of glycolytic enzymes, including adenine nucleotides, inorganic phosphates, and glutathione. Metabolites with asterisks indicate allosteric effectors of glycolytic enzymes. The mathematical model developed in this paper is composed of 46 enzymatic reactions, 11 membrane transport or ion pump systems, 37 reversible binding processes, and 1 allosteric hemoglobin transition. The model includes 61 metabolic intermediates whose steady-state levels are shown schematically in Table 1 and 36 protein-metabolite or protein-protein complexes as variables. In this figure the reactions indicating the catalytic processes of HK, PFK, and PK are described as apparently irreversible ones by a one-headed arrow for the principles of thermodynamics (44), whereas the kinetic equations used in the model are reversible in reality (see the supplemental data).

in the T-state rather than the R-state (8). BIII also binds to PFK (9), aldolase (ALD) (10), glyceraldehyde-3-phosphate dehydrogenase (GAPDH) (11), and lactate dehydrogenase (LDH) (12). Recent observations have shown that these enzymes reduce their catalytic activities upon binding to BIII, and activity is recovered upon dissociation from BIII as free forms (13, 14). These results led us to hypothesize that Hb stabilized in the T-state upon hypoxia serves as a trigger to increase the activity of glycolytic enzymes and to accelerate glucose consumption to increase ATP synthesis. Several reports to date have provided circumstantial evidence showing hypoxia-induced activation of glycolysis by measuring glycolytic intermediates in erythrocytes (15, 16). However, the mechanistic features of the coordination and dynamics of sequential glycolytic reactions and the outcomes in terms of alterations in intracellular metabolites are not comprehensively understood.

The aim of this study was to develop a dynamic mathematical model of metabolism in erythrocytes involving the O_2 -sensing mechanisms of Hb, to predict temporal alterations in intracellular metabolites and cellular energetics in response to hypoxia, and to verify the predictions derived from the model through metabolome analyses. The differential equations of metabolic reactions used in the model are partially based on previous mathematical models for glycolytic metabolism in human erythrocytes (17, 18), for the pentose phosphate pathway, and

for adenine nucleotide metabolism (19–22). In contrast to previous models, we first attempted to include the effects of BIII interactions with Hb and the glycolytic enzymes. The effects of inorganic phosphates and adenine nucleotides that could serve as allosteric effectors of glycolysis were included in the model, similar to recent mathematical models of erythrocytes (23, 24). The temporal alterations in metabolites predicted in the updated dynamic mathematical model are in good agreement with results obtained from the metabolome analyses using capillary electrophoresis mass spectrometry, which has recently emerged as a powerful tool for the global analysis of charged metabolites (25, 26). In contrast, the virtual model lacking the effects of the Hb-BIII interaction was unable to reproduce actual alterations in the metabolites, suggesting a pivotal role for this molecular interaction in the maintenance of erythrocyte energetics.

MATERIALS AND METHODS

Mathematical Model of Human Erythrocyte Metabolism—All numerical

calculations were performed using the E-Cell 3 simulation environment (27, 28). The model can be found in the supplemental data. It provides rate equations and the relevant parameters for all processes included in the model.

Description of the Metabolic Model—We developed a mathematical model of human erythrocyte metabolism (Fig. 1) with kinetic descriptions of reaction rates derived from previously published experimental data and partially from those based on published models, as depicted in detail in the supplemental data. The metabolic reactions included in the developed model are listed in Table 1, and the abbreviations of enzymes and compounds are shown in Tables 1 and 2, respectively. Our mathematical model not only included the glycolytic pathway but also comprised other metabolic pathways that are directly or indirectly related to regulatory mechanisms for glycolysis. The pentose monophosphate shunt, adenine nucleotide metabolism, and the salvage pathway including hypoxanthine-guanine phosphoribosyltransferase were included, since these components determine levels of AMP and P_i , which are known regulators of PFK and GAPDH, respectively (asterisks in Fig. 1). Another important component we included is the *de novo* synthesis and transport of glutathione. This compound occurs at millimolar levels in the cell, and its synthesis and transport are significant energy-consuming processes. Furthermore, GSH serves as a regulator of H.K. The Na^+/K^+ pump consumes large

TABLE 1
Enzymatic reactions included in the model

Enzyme/Process	Abbreviation	Substrates	Products	Effectors
Hexokinase	HK	GLC + MgATP	→ G6P + MgADP	2, 3-BPG, GDP, GSH
Phosphoglucose isomerase	PGI	G6P	↔ F6P	
Phosphofructokinase	PFK	F6P + MgATP	→ F-1,6BP + MgADP	IA TP, Mg, 2, 3-BPG IA MP, Phos, GDP
Aldolase	ALD	F-1,6BP	↔ DHAP + GA3P	
Triose phosphate isomerase	TPI	DHAP	↔ GA3P	
Glyceraldehyde phosphate dehydrogenase	GAPDH	GA3P + Phos + NAD	↔ 1,3-BPG + NADH	
Diphosphoglycerate mutase	DPGM	1,3-BPG	→ 2,3-BPG	
Diphosphoglycerate phosphatase	DPGase	2,3-BPG	→ P3GA + Phos	
Phosphoglycerate kinase	PGK	1,3-BPG + MgADP	↔ P3GA + MgATP	
Phosphoglyceromutase	PGM	P3GA	↔ P2GA	
Enolase	EN	P2GA	↔ PEP	Mg
Pyruvate kinase	PK	PEP + MgADP	↔ PYR + MgATP	IA TP, F-1, 6BP, GDP
Lactate dehydrogenase	LDH	PYR + NADH	→ LAC + NAD	
Lactate dehydrogenase (NADPH)	LDHP	PYR + NADPH	→ LAC + NADP	
Glucose 6-phosphate dehydrogenase	G6PDH	NADP + G6P	→ GL6P + NADPH	MgATP, 2, 3-BPG
6-Phosphogluconolactonase	6PGLase	GL6P	→ GO6P	
6-Phosphogluconate dehydrogenase	6PGODH	GO6P + NADP	↔ RU5P + NADPH + CO ₂	
Transaldolase	TA	S7P + GA3P	→ E4P + F6P	
Transketolase I	TKI	X5P + R5P	→ GA3P + S7P	
Transketolase II	TK2	X5P + E4P	→ GA3P + F6P	
Ribose-5-phosphate isomerase	R5PI	RU5P	→ R5P	
Xylose-5-phosphate isomerase	X5PI	RU5P	→ X5P	
γ-Glutamyl cysteine synthetase	L_GCS	MgATP + glutamate + cysteine	↔ MgADP + L_GC + Phos	GSH
Glutathione synthetase	GSH_S	L_GC + glycine + MgATP	↔ GSH + MgADP + Phos	
Glutathione reductase (NADPH)	GSSGR	GSSG + NADPH	→ GSH + NADP	
Adenosine deaminase	ADA	ADO	↔ INO	
Adenine phosphoribosyl transferase	ADPRT	ADE + PRPP	→ IA MP + 2Phos	
Adenosine kinase	AK	ADO + MgATP	→ MgADP + IA MP	
Adenosine monophosphate deaminase	AMPDA	IA MP	→ IMP	
AMP phosphohydrolase	AMPase	IA MP	↔ ADO + Phos	
Adenylyl kinase	APK	IA DP + MgADP	↔ IA MP + MgATP	
Hypoxanthine-guanine phosphoril transferase	HGPRT	PRPP + HX _i	→ IMP + 2Phos	
Inosine monophosphatase	IMPase	IMP	↔ INO + Phos	
Purine nucleotide phosphorylase	PNPase	INO + Phos	→ HX _i + R1P	
Phosphoribosyl pyrophosphate synthetase	PRM	RIP	→ R5P	
Phosphoribosyl pyrophosphate synthetase	PRPPsyn	R5P + MgATP	→ PRPP + IA MP + Mg	
Adenosine triphosphate phosphohydrolase	ATPase	MgATP	→ MgADP + Phos	
Glutathione turnover	OX	2GSH	→ GSSG	
Non-glycolytic NADH consumption process	OXNADH	NADH	→ NAD	
Adenine transport process	ADEtr	ADE	→ ADEe	
Adenosine transport process	ADOtr	ADO	→ ADOe	
Hypoxanthine transport process	HXtr	HX _i	→ HXe	ADEe
Inosine transport process	INOtr	INO	→ INOe	
Leak of potassium	K_Leak	Ke	↔ Ki	
Lactate transport process	LACtr	LAC	↔ LACe	
Sodium/potassium pump	NaK_Pump	3Na _i + 2Ke + MgATP	→ 3Na _e + 2Ki + MgADP + Phos	
Leak of sodium	Na_Leak	Na _e	→ Na _i	
Pyruvate transport process	PYRtr	PYR	→ PYRe	
Inorganic phosphate transport process	Phostr	Phos	→ Phose	
GSSG transport process	GSSG transport	GSSG + MgATP	↔ GSSGe + MgADP + Phos	

amounts of MgATP and is modeled using precise kinetic equations described elsewhere. We also considered the effects of magnesium ion (Mg²⁺) binding to ATP, ADP, AMP, 1,3-BPG, 2,3-BPG, F1,6BP, and GDP using the respective binding affinities shown in the supplemental Table 1. Because it is now assumed that enzymes employ the complexed form of ATP (MgATP or MgADP) as substrates, these binding processes are important to be considered. Transport of metabolites such as Ade, Ado, Ino, hypoxanthine, and lactate were modeled under the assumption that they move across the membrane simply according to their concentration gradient between intra- and extracellular spaces. Thus, the diagram shown in Fig. 1 constitutes a mathematical model including 83 different chemical reactions and 11 transporter functions that cover a majority of the metabolic pathways influencing the concentrations of allosteric effectors and/or substrates for glycolysis.

Modeling BIII-mediated Interactions between Hb and Glycolytic Enzymes—Reversible binding of the glycolytic enzymes (PFK, ALD, GAPDH) and two allosteric forms of Hb (R- and T-states) to BIII on the membrane were modeled in the current study on the basis of the individual association constants listed in Table 3. T-state Hb has a 100-fold greater affinity to BIII and is much more likely to associate with this anion transporter than R-state Hb. The catalytic activities of PFK, ALD, and GAPDH are inhibited through their specific binding to BIII, but formation of such complexes appeared to be reversible (13). Based on these findings in the model, these enzymes were assumed to be completely inactivated upon formation of the complex and activated reversibly upon dissociation. Under these circumstances the competitive association of Hb and the glycolytic enzymes with BIII and the resultant changes in glycolysis could occur in response to alterations in partial O₂ tension (pO₂ mm Hg).

A Hypoxia-responsive Model of Erythrocyte Metabolism

TABLE 2

Steady-state concentrations of metabolic intermediates in human erythrocytes in normoxia: concentrations were predicted by the model and observed *in vivo*

Metabolite	Abbreviation	Concentration	
		Model	Literature
Glucose 6-phosphate	G6P	6.0E-02	3.8E-02 ^a , 3.9E-02 ^b
Fructose 6-phosphate	F6P	1.9E-02	1.6E-02 ^a
Fructose 1,6-bisphosphate	F-1,6BP	5.6E-03	7.6E-03 ^a , 2.7E-03 ^b
Dihydroxyacetone phosphate	DHAP	1.5E-02	1.4E-02 ^a
Glyceraldehyde 3-phosphate	GA3P	3.6E-03	4.0E-03 ^a , 5.7E-03 ^b
1,3-Bisphosphoglycerate	1,3-BPG	2.3E-04	4.0E-04 ^a
3-Phosphoglycerate	3PG	4.8E-02	4.5E-02 ^a , 5.4E-02 ^b
2-Phosphoglycerate	2PG	1.4E-02	1.4E-02 ^a
Phosphoenolpyruvate	PEP	8.1E-03	1.7E-02 ^a
Pyruvate	PYR	5.2E-02	5.0E-02 ^a , 7.7E-02 ^b
Lactate	LAC	1.3E+00	1.1E-03 ^a , 1.4E-03 ^b
Gluconolactone 6-phosphate	GL6P	5.3E-06	
Gluconate 6-phosphate	GO6P	4.5E-02	
Ribulose 5-phosphate	RU5P	4.9E-03	
Sedoheptulose 7-phosphate	S7P	2.1E-02	
Xylulose 5-phosphate	X5P	9.0E-03	
Erythrose 4-phosphate	E4P	4.5E-04	
Ribose 5-phosphate	R5P	5.8E-03	
Ribose 1-phosphate	R1P	8.1E-02	6.0E-02 ^a
5-Phosphoribosyl 1-phosphate	PRPP	1.4E-03	5.0E-03 ^a
Inosine monophosphate	IMP	8.1E-03	5.7E-03 ^a
Inosine	INO	1.5E-04	1.0E-03 ^a
Adenine	ADE	1.5E-02	1.3E-02 ^a
Adenosine	ADO	4.5E-05	
Hypoxanthine	HX	1.6E-03	2.0E-03 ^a
L-glutamyl cysteine	L_GC	4.2E-04	
Glutathione (reduced)	GSH	3.3E+00	3.2E+00 ^{a,b}
Glutathione (oxidized)	GSSG	4.7E-03	6.0E-03 ^b
Nicotinamide adenine dinucleotide	NAD	6.5E-02	6.2E-02 ^a
Nicotinamide adenine dinucleotide	NADH	2.8E-04	
Nicotinamide adenine phosphate	NADP	6.5E-05	
Nicotinamide adenine phosphate	NADPH	6.5E-02	6.6E-02 ^a
Potassium ion	Ki	1.3E+02	1.4E+02 ^b
Sodium ion	NaI	3.4E+01	1.0E+01 ^a
Inorganic phosphate	Phos	1.0E+00	1.0E+00 ^b
Total adenosine diphosphate	tADP	3.3E-01	3.1E-01 ^b
Total adenosine monophosphate	tAMP	3.4E-02	3.0E-02 ^b
Total adenosine triphosphate	tATP	1.9E+00	2.1E+00 ^b
Total 2,3-bisphosphoglycerate	t2,3-BPG	3.7E+00	4.5E+00 ^a

^a Reported by Joshi and Palsson (22).

^b Reported by Mulquiney and Kuchel (24).

^c From Ref. 45.

^d From Ref. 46.

^e From Ref. 47.

TABLE 3

Association constants of Hbs and glycolytic enzymes to BIII

Proteins	K _a
	/M
Deoxy-Hb	10000 ^a
Oxy-Hb	100 ^a
PFK	5,000,000 ^b
ALD	1,000,000 ^c
GAPDH	2,000,000 ^c

^a From Ref. 48.

^b From Ref. 49.

^c From Ref. 40.

Thus, in this mathematical model we were able to manipulate pO₂, an independent variable of the model, as a parameter and to predict glycolytic metabolism as a dependent variable. Another important assumption is that pO₂ alters the T-R transition of Hb according to a reversible Hill-type equation (29) that is also dictated by pCO₂ levels, intracellular pH, concentrations of 2,3-BPG and ATP, and temperature (supplemental data, page 8–9).

Perturbations Mimicking Hypoxia—The aforementioned mathematical model was able to stably achieve individual

steady states under varied pO₂ conditions over the range of 0–100 mm Hg. Because we aimed to predict metabolic alterations in response to hypoxia with this model, pO₂ was initially set to 100 mm Hg, a physiological value in alveoli (30). Under these conditions the basal and initial steady-state concentrations were calculated by this model, as depicted in Table 2 and supplemental Table 2. The external parameters, including environmental concentrations of metabolites and initial settings in the model, are listed in supplemental Table 3. To adapt the model to hypoxic conditions, pO₂ was reduced to 30 mm Hg, a value measured in capillary microvessels *in vivo* (30, 31), for the desired lengths of time. As seen in previous studies (30, 31), circulating erythrocytes may be exposed to such a pO₂ value when they travel through capillaries under physiological conditions (30) or when they traverse low-flow or static microvessels belonging to post-ischemic damaged regions in the liver (31). This protocol allowed us to remodel glycolytic metabolism in erythrocytes for the aforementioned circumstances.

Preparation of Human Erythrocytes for CE-MS Analysis—Erythrocytes were isolated from heparinized venous blood sam-

A Hypoxia-responsive Model of Erythrocyte Metabolism

ples collected from healthy male volunteers according to our previous methods (31). Briefly, the samples were centrifuged at $2000 \times g$ at 4°C for 10 min, and the cells were washed 3 times and suspended in Tris buffer, pH 7.4, to adjust hematocrit values to 15%. The cell suspension was divided into hypoxic and normoxic groups. For the hypoxic group the cells were incubated in a gas-tight glass bottle and followed by a gentle purge with highly purified argon gas for 45 min at 4°C . Cell samples (2 ml) were transferred to glass tubes on ice in an O_2 -excluding chamber and finally incubated at 37°C for 0, 0.5, 1, and 3 min. The reactions were terminated by cooling the sample-containing glass tubes with ice-cold water at 4°C . The cells for normoxic controls were incubated similarly to the hypoxic group but treated by purging for 45 min with air instead of argon gas and finally incubated at 37°C for 0, 0.5, 1, and 3 min. Likewise, the reactions were terminated at 4°C by cooling in ice-cold water. For measurements at 0 min, the cells were incubated at 37°C and immediately treated on ice to terminate the reaction. The present protocol for treating erythrocytes with argon gas allowed us to set up reproducible hypoxic conditions where the pO_2 was ~ 30 mm Hg.

The cell samples for these two groups were purified by centrifuging at $2000 \times g$ at 4°C for 10 min, and the pellets were treated with 0.16 ml of cold methanol containing $300 \mu\text{M}$ L-methionine sulfate for deproteinization. L-Methionine sulfate was used as the internal standard to validate the recovery or loss of metabolites during sample preparation and CE-MS analysis (25). Next, 0.16 ml of chloroform and 0.08 ml of distilled water was added and thoroughly mixed. The solution was centrifuged at $12,000 \times g$ at 4°C for 15 min, and the upper aqueous layer was filtered through a centrifugal filter (Millipore 5-kDa NMWL) to remove proteins. The filtrate was analyzed by CE-MS. Metabolome data collected from erythrocytes exposed to hypoxia for the aforementioned times were plotted as relative concentrations versus the 3-min normoxic controls (see below). In some experiments erythrocytes were pretreated by an incubation with buffer saturated with CO , a stabilizer of R-state Hb. This incubation was performed for 20 min before the 45-min normoxic incubation time at 4°C .

In a separate sets of experiments we examined the effects of the aforementioned procedure of hypoxia on the conversion of $[^{13}\text{C}_6]\text{glucose}$ to $[^{13}\text{C}_3]\text{lactate}$ in human erythrocytes. In these experiments erythrocytes isolated from venous blood samples were suspended in buffer to adjust hematocrit values to 30%. The cell suspension was divided into hypoxic and normoxic samples to be treated by purging for 45 min at 4°C with argon and air, respectively. Cell samples (1 ml) were then transferred to glass tubes containing 1 ml of buffer containing 5 mM $[^{13}\text{C}_6]\text{glucose}$, giving a final hematocrit value of 15%. Immediately after mixing at 4°C , the samples were incubated at 37°C for 3 min, and the reactions were terminated at 4°C by immersion in ice-cold water. Preparation of cell pellets and samples to determine the amount of $[^{13}\text{C}_3]$ -labeled lactate was identical to that for conventional metabolome analyses, as described below and elsewhere (26). The flux indicating the conversion of $[^{13}\text{C}_6]\text{glucose}$ to $[^{13}\text{C}_3]\text{lactate}$ was determined as values relative to the amount of L-methionine sulfate in the samples added as

an internal control. Using the same samples, $[^{13}\text{C}_3]2,3\text{-BPG}$ was also determined when necessary.

Sample Recovery of Metabolome Analysis by CE-MS—Hb has the ability to capture intracellular metabolites such as 2,3-BPG and ATP. Additionally, deproteinization with cold methanol before processing for CE-MS analysis could cause loss of some of these metabolites through binding to denatured Hb. To quantify the putative loss of such metabolites, 2,3-BPG, ATP, glucose 6-phosphate (G6P), lactate, or α -ketoglutarate were incubated for 3 min at a final concentration of $300 \mu\text{M}$ (2,3-BPG) or $100 \mu\text{M}$ (other metabolites) in buffer containing $300 \mu\text{M}$ purified human Hb. To examine differences in the loss of these metabolites between T- and R-state Hb, the sample mixture was purged for 60 min with purified argon gas or with air, respectively, in the presence of 1 mg/ml sodium dithionite. Purified Hb solution was generously provided by Oxygenix Co. Ltd., Tokyo, Japan. The samples for CE-MS analysis were prepared as described above.

Instrumentation—All CE-MS experiments were performed using an Agilent CE Capillary Electrophoresis System equipped with an air pressure pump, an Agilent 1100 series MSD mass spectrometer and an Agilent 1100 series isocratic high performance liquid chromatography pump, a G1603A Agilent CE-MS adapter kit, and a G1607A Agilent CE-MS sprayer kit (Agilent Technologies). System control, data acquisition, and MSD data evaluation were performed using G2201AA Agilent ChemStation software for CE-MSD.

CE-MS Conditions for Anionic Metabolites—A cationic polymer coated SMILE (+) capillary was obtained from Nacalai Tesque (Kyoto, Japan) and used as the separation capillary ($50\text{-}\mu\text{m}$ inner diameter \times 100-cm total length). The electrolyte for the CE separation was 50 mM ammonium acetate solution, pH 8.5. Samples were injected with a pressure injection of 50 mbar for 30 s (30 nl). The applied voltage was set at -30 kV . ESI-MS was conducted in the negative ion mode, and the capillary voltage was set at 3500 V . For MS using the selective ion monitoring mode, deprotonated $[\text{M}-\text{H}]^-$ ions were monitored for anionic metabolites of interest (32).

CE-MS Conditions for Nucleotides and Coenzyme A Compounds—Separations were carried out on a gas chromatograph capillary, polydimethylsiloxane (DB-1) ($50\text{-}\mu\text{m}$ inner diameter \times 100-cm total length) (Agilent Technologies). The electrolyte for the CE separation was 50 mM ammonium acetate, pH 7.5. The applied voltage was set at -30 kV , and a pressure of 50 mbar was added to the inlet capillary during the run to maintain a conductive liquid junction at the capillary outlet. All other conditions were the same as in the anionic metabolite analysis (32).

Calculation of Energy Charge in the Mathematical Model—Based on the definition proposed by Atkinson and Walton, an energy charge was calculated as an index of contents of high energy phosphate bonds in adenylate in the BIII(+) and BIII(-) models (33, 34). Energy charge is defined as one-half the number of anhydride-bound phosphates per adenylate moiety: energy charge = $(\text{ATP} + \frac{1}{2}\text{ADP})/(\text{AMP} + \text{ADP} + \text{ATP})$. With this parameter, the energy potential of an erythrocyte may vary from 0 to 1.

A Hypoxia-responsive Model of Erythrocyte Metabolism

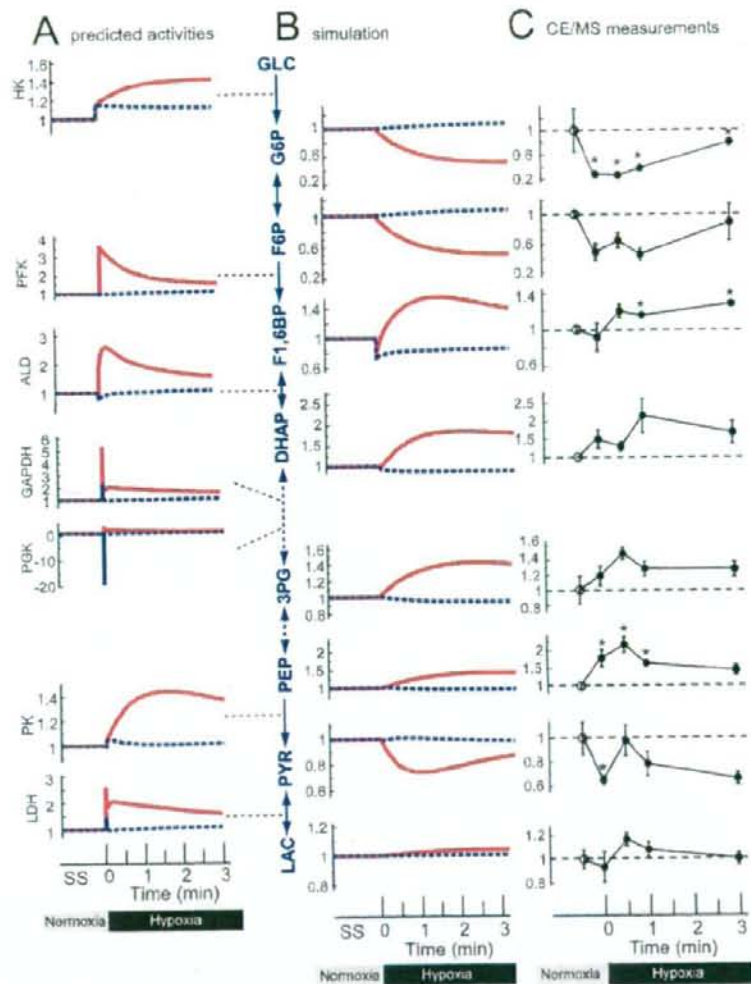


FIGURE 2. Prediction of hypoxia-induced alterations in activities of glycolytic enzymes and in levels of their products in the mathematical model and demonstration by CE-MS analysis in human erythrocytes. *A*, hypoxia-induced changes in predicted activities of glycolytic enzymes. *B*, predicted concentrations of glycolytic products. *Red* and *blue* lines indicate results of the simulation with and without inclusion of the BIII-Hb interactions, respectively. *C*, hypoxia-induced alterations in the relative concentrations of the products determined by CE-MS analysis. *Closed circles* indicate ratios of hypoxic metabolite concentrations to normoxic control concentrations, which are represented with *open circles*. Values are the mean \pm S.E. of four separate experiments. Asterisks, $p < 0.05$ versus the steady-state base-line values.

Statistical Analyses—Differences in mean values among groups in the metabolome analyses were examined statistically using a one-way analysis of variance and Fisher's multiple comparison test.

RESULTS

Modeling the BIII-Hb Interaction Enhances Hypoxia-induced Activation of Glycolysis—Fig. 2*A* illustrates the differences in temporal alterations in the enzyme activities between the model involving BIII interactions with Hb and the glycolytic enzymes (BIII(+)) model; *red solid line* and the model without these interactions (BIII(-)) model; *blue dotted line* during the

3-min virtual hypoxia. Overall, the activities of glycolytic enzymes in the BIII(+)) model were stimulated to greater extents than those in the BIII(-)) model (Fig. 2*A*). The activity of HK, which mediates the initial reaction in glycolysis, was initially equally elevated upon hypoxia in the two models. Putative mechanisms for this increase will be mentioned under "Discussion." HK activity in the BIII(+)) model exhibited further activation compared with the BIII(-)) model; this difference appeared to result from a decrease in G6P (*uppermost panel* in Fig. 2*B*) and an increase in ATP, leading to a disappearance of HK product inhibition. Such an activation process is likely to help accelerate the initial step of glycolysis, as discussed below. As expected, the activities of PFK, ALD, and GAPDH, enzymes mediating the intermediate steps in glycolysis, modeled as BIII-binding enzymes, spiked immediately as a result of their release from BIII upon Hb binding. In contrast, the activity of these enzymes did not change greatly in the BIII(-)) model, with the exception of GAPDH, which was elevated modestly but noticeably in the BIII(-)) model. This elevation appeared to result from a decrease in 1,3-BPG, a product of the enzyme, through its binding to T-state Hb, as described in the model in supplemental Table 1. Other important differences to be noted in the BIII(+)) model were the disappearance of the decreased activity of PGK and the marked activation of PK, whereas the activities of these ATP-generating enzymes were not predicted to contribute to acceleration of glycolysis in the

BIII(-)) model. The LDH activity was elevated in both models, but the elevation was substantially higher and sustained to a greater extent in the BIII(+)) model compared with the BIII(-)) model. As a result the temporal pattern of LDH activity in the BIII(+)) model was similar to that of GAPDH. This behavior is due to the fact that NADH, a product of GAPDH, determines the activity of LDH. The predicted level of glycolytic metabolites indicated a unique profile in the BIII(+)) model. In the BIII(-)) model, G6P and F6P increased slightly, whereas F1,6BP, DHAP, 3PG, and PEP decreased modestly versus the steady-state base-line levels (Fig. 2*B*). In contrast, the BIII(+)) model displayed a pattern opposite to the BIII(-)) model, with

A Hypoxia-responsive Model of Erythrocyte Metabolism

decreases in G6P and F6P by 50% and increases in F1,6BP, DHAP, 3PG, and PEP by 40% versus the corresponding baseline levels. The model predicted that pyruvate decreases, whereas lactate slightly increases in the BIII(+) model. The decrease in pyruvate seemed to result from a prediction by this model that consumption of pyruvate by LDH surpasses production by PK, as judged from the 2.5-fold peak increase in LDH activity versus the relatively modest activation of PK, which peaks at 1.4-fold. Because lactate is modeled to be transported according to a gradient between the intra- and extracellular spaces, elevation of lactate was small even in the BIII(+) model.

Demonstration of Hypoxia-induced Alterations in Glycolytic Products by CE-MS—The aforementioned results from the model raise the possibility that hypoxia-triggered activation of GAPDH drives activation of LDH as a downstream target through NADH generation and thereby facilitates the second half of the glycolytic reactions. Consequently, stimulation of the hypoxia-dependent BIII interaction of the intermediate enzymes (PFK, ALD, GAPDH) contributed to activation of HK as the initial step and that of PK and LDH as the final step in glycolysis in the model as a whole. To examine whether temporal alterations in the glycolytic metabolites of human erythrocytes occur in agreement with those predicted by the BIII(+) model, erythrocytes were exposed to hypoxia for 3 min, and the amounts of various metabolites were determined by CE-MS. As seen in Fig. 2C, G6P and F6P were significantly lower than those measured as steady-state controls under normoxic conditions. In contrast, levels of F1,6BP, DHAP, 3PG, and PEP were significantly greater than normoxic steady-state controls. These results are entirely consistent with those predicted by the BIII(+) model. The absolute concentrations of glycolytic metabolites measured by CE-MS at each time point are shown in supplemental Table 4.

Adsorption of 2,3-BPG and ATP to Hb during Protein Denaturation in Preparation for CE-MS—CE-MS validation of the data predicted by the dynamic mathematical model supported the hypothesis that hypoxia-dependent BIII interactions with PFK, GAPDH, and ALD play a crucial role in systematic activation of glycolytic reactions to support the demand for ATP in erythrocytes. As seen in Fig. 3A, the ATP content of the cells exposed to hypoxia at 4 °C was decreased by 30% versus that measured under normoxic steady-state conditions. This level of ATP was maintained and modestly elevated during the subsequent 3-min hypoxic conditions. Likewise, the content of 2,3-BPG did not decrease in hypoxia but, rather, was elevated during the 3-min hypoxic period. Because these metabolites are known to adsorb to T-state Hb, we examined whether the current protocol for measuring metabolites reflected only the amount of free metabolite (i.e. that not bound to Hb) or the total amount in the cells. As seen in Fig. 3B, the presence of free T-state Hb, stabilized by dithionite, but not free R-state Hb, stabilized under normoxia without dithionite, caused apparent decreases in ATP and 2,3-BPG contents but not in G6P, lactate, and 2-oxoglutarate contents. Approximately 30% of the ATP and 90% of the 2,3-BPG were lost during the protein denaturation step before CE-MS.

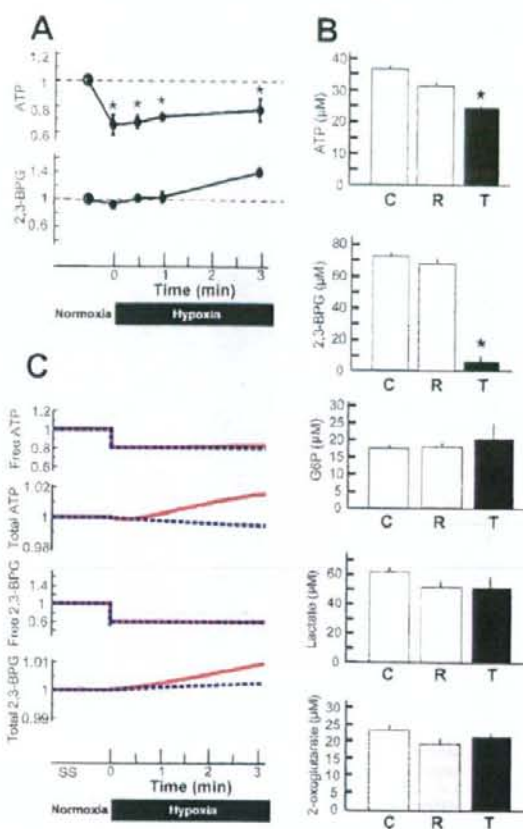


FIGURE 3. Hypoxia-induced alterations in measured concentrations of ATP and 2,3-BPG and effects of the presence of Hb on measurements of metabolites by CE-MS. Panel A, hypoxia-induced changes in measured concentration of ATP and 2,3-BPG. Panel B, influence of the presence of Hb. C, standard measurements in the Hb-free buffer; R and T, measurements in Hb-containing buffer under ambient and hypoxic conditions, respectively. Data shown are the means \pm S.D. of three separate experiments. * $p < 0.05$ versus the R group. Panel C, prediction indicating temporal alterations in free and total ATP and 2,3-BPG in the model. Red lines, data collected from the BIII(+) model. Blue dotted lines, data collected from the BIII(-) model.

These results suggest that in the cell-free protein solution the ATP and 2,3-BPG data obtained from CE-MS could be underestimated because CE-MS only takes into account free metabolite contents and neglects the Hb-bound forms of these metabolites. On the other hand in the case of the cell-containing system, the T-state of Hb in the hypoxia-exposed erythrocytes could be easily stabilized into the R-state (35) during centrifugation at low temperatures before protein denaturation; such a process before sample processing could stimulate the release of 2,3-BPG adsorbed to Hb under hypoxic conditions. Considering the above, we compared the CE-MS data for ATP and 2,3-BPG with the predicted data for free and total amounts of these metabolites obtained from the model. As seen in Fig. 3C, the temporal profile of free ATP in the model was in good agreement with the CE-MS results for ATP shown in Fig. 3A. The amounts of

A Hypoxia-responsive Model of Erythrocyte Metabolism

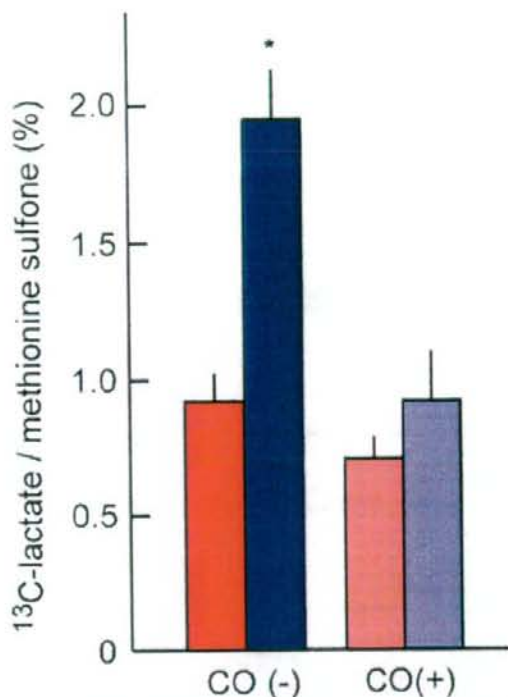


FIGURE 4. Hypoxia-induced acceleration of glycolysis assessed by pulse-chase analysis of the conversion of [¹³C]glucose to [¹³C]lactate in human erythrocytes and its blockade by CO. Red and blue bars indicate relative amounts of [¹³C]lactate generated per 1 min after loading with [¹³C]glucose at 5 mM under normoxic and hypoxic conditions, respectively. CO(-), control erythrocytes not treated with CO. CO(+), CO-pretreated erythrocytes. Methionine sulfone is an internal standard that was added at 100 μM to protein-free samples for CE-MS collected from the erythrocyte lysates. Means ± S.E. of 3–4 separate experiments are shown. *, *p* < 0.05 versus normoxic controls (CO(-)).

total ATP in the model were modestly elevated. On the other hand the prediction of the temporal profile of free 2,3-BPG, whose adsorption is dictated by the T-state of Hb, displayed an abrupt drop compared with the steady-state base-line value. This difference with respect to the CE-MS data (Fig. 3A) is not surprising when the aforementioned effect of low temperature on 2,3-BPG release from the T-state of Hb is taken into consideration. In the model prediction the amount of total 2,3-BPG gradually increased with time, suggesting that the drop in free 2,3-BPG predicted in the model does not result from down-regulation of its synthesis but from its adsorption to Hb. This was demonstrated by the [¹³C₆]glucose pulse-chase measurements described below.

Hypoxia Induces Acceleration of Glycolysis in Human Erythrocytes—The results of the metabolome analyses (Figs. 2 and 3) suggest that hypoxia causes activation of glycolysis. To examine whether the actual flux of glycolysis could be accelerated in response to hypoxia, we determined the rate of conversion of [¹³C]glucose into [¹³C]lactate in human erythrocytes. As seen in Fig. 4, the rate of production of [¹³C]lactate was accelerated 1.8-fold within 1 min after exposure to hypoxia. In contrast, pretreatment of the cells

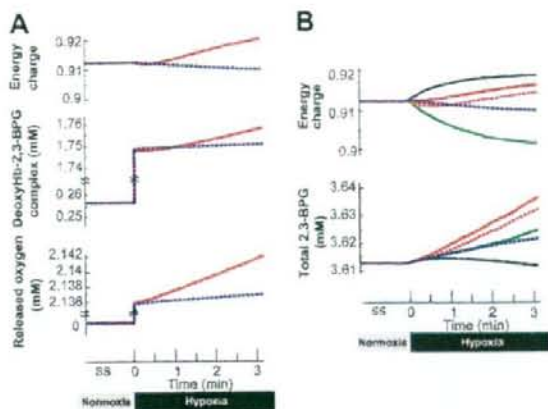


FIGURE 5. Beneficial effects of BIII-Hb interactions on cellular energetics and Hb allosteric predicted by the mathematical model. A, hypoxia-induced alterations in the values of energy charge which is defined by (ATP + 0.5ADP)/(AMP + ADP + ATP). B, the sensitivity analysis indicating changes in energy charge (upper) and 2,3-BPG (lower) generation under different hypoxic conditions when the amounts of the following enzymes were increased by 2-fold: PFK + ALD + GAPDH (red), none (same as BIII(-) model) (blue), HK (green), PFK (broken red), and PK (black). Note that HK activation results in a decrease in energy charge and an increase in 2,3-BPG generation, whereas PK activation alone increases energy charge without stimulating 2,3-BPG generation, suggesting that activation of PFK or PFK + ALD + GAPDH leads to simultaneous increases in energy charge and 2,3-BPG generation in the model.

with CO to stabilize Hb in the R-state attenuated the hypoxia-induced acceleration of lactate production almost completely. These results suggest that the hypoxia-induced stabilization of T-state Hb plays a crucial role in triggering glycolytic activation in erythrocytes.

The Model Including BIII-Hb Interaction Predicts Sustained Energy Charge and Accelerated O₂ Release—Using the dynamic mathematical model validated by CE-MS analysis, we examined the roles of the BIII-Hb interaction in regulation of cellular energetics and O₂ delivery. As an index of the content of high energy phosphate bonds of adenylate nucleotides, an energy charge was calculated for the BIII(+) and BIII(-) models. As seen in the upper panel of Fig. 5A, the basal energy charge under normoxic steady-state conditions was 0.91. This value, obtained by the model prediction, was comparable with that reported in previous studies ranging from 0.86 (36) to 0.935 (37), supporting the hypothesis that the BIII(+) model is consistent with the real metabolic behavior of human erythrocytes. Upon exposure to hypoxia, the BIII(+) model exhibited further increases in the energy charge and in the amounts of the deoxy-Hb-2,3-BPG complex (Fig. 5A). Under these circumstances the amounts of O₂ released from the cell is greater in the BIII(+) model than in the BIII(-) model.

Based on the predictions of the mathematical model shown in Fig. 5A as well as in Fig. 3C, we also examined differences in the conversion of glucose to 2,3-BPG between normoxic and hypoxic cells under the same experimental conditions as in Fig. 4. The ratios of [¹³C₃]2,3-BPG/methionine sulfone were 2.1 ± 0.3 and 5.4 ± 0.2% (mean ± S.E. of 1-min incubations in 4 separate experiments) under nor-

moxic and hypoxic conditions, respectively, indicating a significant acceleration in *de novo* 2,3-BPG synthesis upon hypoxia. Considering the CE-MS data in Fig. 3A, indicating maintenance of free 2,3-BPG in erythrocytes, the results achieved by the model were consistent with the hypothesis that the BIII-Hb interaction contributes greatly to the delivery of 2,3-BPG to Hb to stabilize the T-state and, thereby, to sustain the release of O₂ in hypoxic conditions.

In Fig. 5B, we conducted sensitivity analysis to determine whether or not the amount of any particular enzyme making up the glycolytic pathway could alter the effectiveness of the sustained increase in energy charge and 2,3-BPG generation during hypoxia in the model. We, therefore, increased the amount of each glycolytic enzyme in the pathway by 2-fold simultaneously with hypoxia. As shown in Fig. 5B, HK activation (green line in panel B) resulted in a decrease in energy charge and an increase in 2,3-BPG, whereas PK activation (black in panel B) increased energy charge without stimulating 2,3-BPG generation. On the other hand, activation of PFK (broken red in panel B) or PFK+ALD+GAPDH (red in panel B) led to simultaneous elevation of energy charge and 2,3-BPG generation in the model. These analyses suggest that activation of enzymes situated midway through the glycolytic pathway positively regulate energy charge and 2,3-BPG generation simultaneously in erythrocytes. The results lend further support to the notion that sustained elevation of 2,3-BPG and the resultant increase in O₂ release predicted by the model are likely to be metabolically relevant.

DISCUSSION

Glycolysis involves a series of enzymatic reactions to couple glucose oxidation to generation of ATP. On the basis of previous studies (for metabolism (21, 24) and for BIII-enzymes/Hb interactions (13, 14)), the BIII(+) model simulated dynamic alterations in enzyme activities and the corresponding metabolites using the assumption that the intermediate glycolytic enzymes, such as PFK, GAPDH, and ALD, bind to R-state Hb in their quiescent form and become activated upon their release from T-state Hb in response to hypoxia. The model predictions developed in this study clearly indicate that such an activation of the intermediate enzymes triggered by hypoxia-induced stabilization of T-state Hb not only induces acceleration of the flux of metabolites through the glycolytic reactions but also triggers activation of the initial and final steps of glycolysis as a result of alterations in the corresponding allosteric effectors (e.g. 2,3-BPG for HK) and levels of substrates and products (e.g. ATP and G6P for HK, NADPH for LDH).

As a consequence, PGK and PK, the glycolytic enzymes for ATP synthesis, are predicted to be accelerated upon hypoxia. The predicted hypoxia-induced remodeling of glycolytic enzyme activities results in decreases in upstream products such as G6P and F6P and increases in the intermediate products such as F1,6BP, DHAP, 3PG, 2,3-BPG, and PEP. Furthermore, these predicted alterations in glycolytic products were actually demonstrated by CE-MS analysis in human erythrocytes. These results indicate that the mathematical model described in this study is capable of predicting hypoxia-

induced remodeling of energy metabolism, suggesting a physiological significance of the BIII-Hb interaction in accelerating glycolysis in erythrocytes upon exposure to hypoxia.

The sensitivity analysis, showing that the activation of these glycolytic enzymes altered hypoxia-induced responses of metabolites, led us to suggest that the alterations in metabolites determined by CE-MS are comparable with those elicited by about a 2–5-fold increase in the amounts of PFK (supplemental Fig. 1A). On the other hand the increases in ALD and GAPDH apparently had little or no effect on glycolytic activation. However, careful analysis of the sensitivity data (supplemental Fig. 1, A–C) indicates that increases in the latter two enzymes obviously contributed to the spike in the activation of LDH. It is worthwhile noting that such an initial LDH spike is observed in Fig. 2A but not in supplemental Fig. 1A, where only PFK is activated. Thus, these simulations collectively suggest that PFK activation plays a major role, whereas activation of ALD and/or GAPDH *per se* plays a minimal role. This does not exclude, however, a cooperative effect of these two latter enzymes in PFK activation for the stimulation of downstream reactions in the glycolytic pathway, which may be of physiologic and metabolic importance.

Our results show the predicted time-dependent alterations in concentrations of metabolites and the demonstration by CE-MS of these changes. The changes are physiologically relevant to previous observations of hypoxia-elicited metabolic responses in human erythrocytes. For instance, the change in G6P could not only influence glycolysis but also regulate other metabolic pathways. In the BIII(+) model, but not in the BIII(-) model, G6P decreased rapidly after the onset of hypoxia. Because this metabolite serves as a substrate for G6PDH, the rate-limiting step of the pentose phosphate pathway, such a change in G6P could rapidly limit the flux of metabolites through this pathway. We were unable to detect a decrease in the flux of [¹³C]glucuronolactone, the product of G6PDH, presumably because the changes were insufficient to be detected by CE-MS. However, the hypothesis is well supported by previous observations that hypoxia causes down-regulation of the pentose phosphate pathway, in parallel with an acceleration in glycolysis in erythrocytes (38). Second, erythrocytes exposed to hypoxia have been known to release ATP into the extracellular space, which results in endothelium-dependent vasorelaxation of arterioles (3, 39, 41). Considering that the K_m of the purinergic receptor for ATP is in the submicromolar range, the amount of ATP released from erythrocytes appears to be far smaller than levels normally found in the intracellular spaces. Despite the fact that the time needed to transit through the organ microvascular systems is thought to be in the range of several seconds, erythrocytes could undergo hypoxia frequently during their passage through the capillaries. In some organs (e.g. liver) erythrocytes exhibit transitory stasis among the capillary networks (42, 43). Under these circumstances glycolytic acceleration triggered by the BIII-Hb interaction could greatly enhance the maintenance of intracellular ATP levels.

A Hypoxia-responsive Model of Erythrocyte Metabolism

In this context acceleration of glucose oxidation upon exposure to hypoxia is likely to be necessary to maintain the functional integrity of erythrocytes through at least two different aspects; that is, supplementation of ATP and sustained stabilization of T-state Hb by 2,3-BPG, an allosteric effector generated through a side reaction in glycolysis. Judging from the CE-MS measurements shown in Fig. 3A, the free amounts of ATP and 2,3-BPG were not apparently reduced during the 3-min hypoxia. Considering that deoxy-Hb has a greater ability to absorb these metabolites than oxy-Hb, these results led us to hypothesize that *de novo* synthesis of these metabolites is dramatically up-regulated during even short periods of hypoxia. Evidence to support this hypothesis was well documented by the CE-MS measurements, indicating accelerated conversion of ^{13}C -labeled glucose into 2,3-BPG and lactate under hypoxic conditions. As predicted by the mathematical model in Fig. 5A, such an acceleration of 2,3-BPG synthesis is likely to contribute to a rapid increase in the Hb-2,3-BPG complex that could consequently lead to the release of residual Hb-bound O_2 from erythrocytes.

Through further analyses of the model depicted in Fig. 5B, we suggest that PFK activation is a crucial step for the up-regulation of both energy charge and 2,3-BPG generation, whereas activation of the initial (e.g. HK) or final (e.g. PK) steps of the glycolytic pathway fails to satisfy these requirements. Furthermore, activation of ALD or GAPDH with that of PFK appears to help activate LDH at the onset of hypoxia. Whether the amounts of O_2 released from the cells through these putative mechanisms are sufficient to fulfill tissue O_2 demand should be further examined *in vivo*.

In this model several of the components of real erythrocytes are missing. For instance, hypoxia-induced switching between BIII and three glycolytic enzymes is simply based on their individual association constants for binding to BIII. On the other hand, a previous report suggested that these enzymes behave as a macromolecular complex for the execution of glycolysis (13). Because pH effects on Hb allostery were not included in the current model, the disparity in O_2 saturation between BIII(+) and BIII(-) models could in reality be greater than that calculated in this study. In addition, the initial environmental conditions governing external metabolite concentrations (e.g. lactate in the extracellular space) could be altered under disease conditions. Such an alteration, however, did not change the prediction of hypoxia-induced glycolytic remodeling *in silico* (supplemental Fig. 2). With regard to these considerations, the model needs to be further refined by including the function of carbonic anhydrase, an enzyme that senses tissue CO_2 (6). This would be very helpful when it comes to applying the current model for the prediction of time-dependent alterations in erythrocyte metabolism under chronically hypoxic conditions.

REFERENCES

- Murphy, J. R. (1960) *J. Lab. Clin. Med.* **55**, 286–302
- Lenfant, C., Torrance, J., English, E., Finch, C. A., Reynafarje, C., Ramos, J., and Faura, J. (1968) *J. Clin. Invest.* **47**, 2652–2656
- Ellsworth, M. L., Forrester, T., Ellis, C. G., and Dietrich, H. H. (1995) *Am. J. Physiol.* **269**, H2155–H2161
- Bergfeld, G. R., and Forrester, T. (1992) *Cardiovasc. Res.* **26**, 40–47
- Jagger, J. E., Bateman, R. M., Ellsworth, M. L., and Ellis, C. G. (2001) *Am. J. Physiol. Heart Circ. Physiol.* **280**, 2833–2839
- Jensen, F. B. (2004) *Acta Physiol. Scand.* **162**, 215–227
- Southgate, C. D., Chishti, A. H., Mitchell, B., Yi, S. J., and Palek, J. (1996) *Nat. Genet.* **14**, 227–230
- Tsuneshige, A., Imai, K., and Tyuma, I. (1987) *J. Biochem. (Tokyo)* **101**, 695–704
- Higashi, T., Richards, C. S., and Uyeda, K. (1979) *J. Biol. Chem.* **254**, 9542–9550
- Murthy, S. N., Liu, T., Kaul, R. K., Kohler, H., and Steck, T. L. (1981) *J. Biol. Chem.* **256**, 11203–11208
- Kliman, H. J., and Steck, T. L. (1980) *J. Biol. Chem.* **255**, 6314–6321
- Harris, S. J., and Winzor, D. J. (1990) *Biochim. Biophys. Acta* **1038**, 306–314
- Campanella, M. E., Chu, H., and Low, P. S. (2005) *Proc. Natl. Acad. Sci. U.S.A.* **102**, 2402–2407
- Chu, H., and Low, P. S. (2006) *Biochem. J.* **400**, 143–151
- Costa, L. E., and De Miranda, I. M. (1976) *Acta Physiol. Latinoam.* **26**, 115–121
- Moore, L. G., and Brewer, G. J. (1980) *Am. J. Phys. Anthropol.* **53**, 11–18
- Rapoport, T. A., and Heinrich, R. (1975) *Biosystems* **7**, 120–129
- Rapoport, T. A., Heinrich, R., and Rapoport, S. M. (1976) *Biochem. J.* **154**, 449–469
- Joshi, A., and Palsson, B. O. (1989) *J. Theor. Biol.* **141**, 515–528
- Joshi, A., and Palsson, B. O. (1989) *J. Theor. Biol.* **141**, 529–545
- Joshi, A., and Palsson, B. O. (1990) *J. Theor. Biol.* **142**, 41–68
- Joshi, A., and Palsson, B. O. (1990) *J. Theor. Biol.* **142**, 69–85
- Mulquaney, P. J., Bubbs, W. A., and Kuchel, P. W. (1999) *Biochem. J.* **342**, 567–580
- Mulquaney, P. J., and Kuchel, P. W. (1999) *Biochem. J.* **342**, 581–596
- Soga, T., Baran, R., Suematsu, M., Ueno, Y., Ikeda, S., Sakurakawa, T., Kakazu, Y., Ishikawa, T., Robert, M., Nishioka, T., and Tomita, M. (2006) *J. Biol. Chem.* **281**, 16768–16776
- Soga, T., Ohashi, Y., Ueno, Y., Naraoka, H., Tomita, M., and Nishioka, T. (2003) *J. Proteome Res.* **2**, 488–494
- Tomita, M., Hashimoto, K., Takahashi, K., Shimizu, T. S., Matsuzaki, Y., Miyoshi, F., Saito, K., Tanida, S., Yugi, K., Venter, J. C., and Hutchison, C. A., III (1999) *Bioinformatics* **15**, 72–84
- Takahashi, K., Yugi, K., Hashimoto, K., Yamada, Y., Pickett, C., and Tomita, M. (2002) *IEEE Intell. Syst.* **17**, 64–71
- Dash, R. K., and Basingthwaite, I. B. (2004) *Ann. Biomed. Eng.* **32**, 1676–1693
- Tsai, A. G., Johnson, P. C., and Intaglietta, M. (2003) *Physiol. Rev.* **83**, 933–963
- Suganuma, K., Tsukada, K., Kashiba, M., Tsuneshige, A., Furukawa, T., Kubota, T., Goda, N., Kitajima, M., Yonetani, T., and Suematsu, M. (2006) *Antioxid. Redox Signal.* **8**, 1847–1855
- Soga, T., Ueno, Y., Naraoka, H., Ohashi, Y., Tomita, M., and Nishioka, T. (2002) *Anal. Chem.* **74**, 2233–2239
- Atkinson, D. E. (1968) *Biochemistry* **7**, 4030–4034
- Atkinson, D. E., and Walton, G. M. (1967) *J. Biol. Chem.* **242**, 3239–3241
- Yonetani, T., Tsuneshige, A., Zhou, Y., and Chen, X. (1998) *J. Biol. Chem.* **273**, 20323–20333
- Komarova, S. V., Mosharov, E. V., Vitvitsky, V. M., and Atullakhanov, F. I. (1999) *Blood Cells Mol. Dis.* **25**, 170–179
- Shimizu, T., Kono, N., Kiyokawa, H., Yamada, Y., Hara, N., Mineo, I., Kawachi, M., Nakajima, H., Wang, Y. L., and Tarui, S. (1988) *Blood* **71**, 1130–1134
- Messana, I., Orlando, M., Cassiano, L., Pennacchietti, L., Zuppi, C., Castagnola, M., and Giardina, B. (1996) *FEBS Lett.* **390**, 25–28
- Sprague, R. S., Ellsworth, M. L., Stephenson, A. H., and Lonigro, A. J. (1996) *Am. J. Physiol.* **271**, H2717–H2722
- von Ruckmann, B., and Schubert, D. (2002) *Biochim. Biophys. Acta* **1559**, 43–55
- Ellsworth, M. L. (2004) *Med. Sci. Sports Exerc.* **36**, 35–41
- MacPhee, P. J., Schmidt, E. E., and Groom, A. C. (1995) *Am. J. Physiol.* **269**, G692–G698
- Hauck, E. F., Apostel, S., Hoffmann, J. F., Heimann, A., and Kempki, O. (2004) *J. Cereb. Blood Flow Metab.* **24**, 383–391

A Hypoxia-responsive Model of Erythrocyte Metabolism

44. Qian, H., and Beard, D. A. (2005) *Biophys. Chem.* **114**, 213–220
45. Magnani, M., Stocchi, V., Piatti, E., Dacha, M., Dallapiccola, B., and Fornaini, G. (1983) *Blood* **61**, 915–919
46. Yamamoto, T., Moriwaki, Y., Takahashi, S., Ishizashi, H., and Higashino, K. (1994) *Horm. Metab. Res.* **26**, 504–508
47. Mills, G. C., Schmalstieg, F. C., Trimmer, K. B., Goldman, A. S., and Goldblum, R. M. (1976) *Proc. Natl. Acad. Sci. U. S. A.* **73**, 2867–2871
48. Walder, J. A., Chatterjee, R., Steck, T. L., Low, P. S., Musso, G. F., Kaiser, E. T., Rogers, P. H., and Arnone, A. (1984) *J. Biol. Chem.* **259**, 10238–10246
49. Jenkins, J. D., Madden, D. P., and Steck, T. L. (1984) *J. Biol. Chem.* **259**, 9374–9378